Molecular Systems Biology (2005) doi:10.1038/msb4100036

www.molecularsystemsbiology.com
Article number: 2005.0028

molecular systems biology

Threshold responses to morphogen gradients by zero-order ultrasensitivity

Gustavo J Melen[1,3], Sagi Levy[1,2,3], Naama Barkai[1,2] and Ben-Zion Shilo[1,*]

[1] Department of Molecular Genetics, Weizmann Institute of Science, Rehovot, Israel and [2] Department of Physics of Complex Systems, Weizmann Institute of Science, Rehovot, Israel
[3] These authors contributed equally to this work
* Corresponding author. Molecular Genetics, Weizmann Institute, Rehovot 76100, Israel. Tel.: +972 8 934 3169; Fax: +972 8 934 4108;
E-mail: benny.shilo@weizmann.ac.il

Received 14.7.05; accepted 27.10.05

Translating a graded morphogen distribution into tight response borders is central to all developmental processes. Yet, the molecular mechanisms generating such behavior are poorly understood. During patterning of the *Drosophila* embryonic ventral ectoderm, a graded mitogen-activated protein kinase (MAPK) activation is converted into an all-or-none degradation switch of the Yan transcriptional repressor. Replacing the cardinal phosphorylated amino acid of Yan by a phosphomimetic residue allowed its degradation in a MAPK-independent manner, consistent with Yan phosphorylation being the critical event in generating the switch. Several alternative threshold mechanisms that could, in principle, be realized by this phosphorylation, including first order, cooperativity, positive feedback and zero-order ultrasensitivity, were analyzed. We found that they can be distinguished by their kinetics and steady-state responses to Yan overexpression. In agreement with the predictions for zero-order kinetics, an increase in Yan levels did not shift the degradation border, but significantly elevated the time required to reach steady state. We propose that a reversible loop of Yan phosphorylation implements a zero-order ultrasensitivity-like threshold mechanism, with the capacity to form sharp thresholds that are independent of the level of Yan.
Molecular Systems Biology 13 December 2005; doi:10.1038/msb4100036
Subject Categories: development; signal transduction
Keywords: Drosophila; EGFR; MAPK; mathematical modeling; morphogen; Pointed/Yan

Introduction

In most developmental contexts, long-range patterning is directed by morphogens, which spread from a restricted source, and diffuse to create a concentration gradient within a field of unpatterned cells. The generation of pattern requires the conversion of this gradient into sharp response borders. Depending on the morphogen level it encounters, a cell must make a clearcut decision whether or not to induce the expression of a given set of target genes. The new interface defined by such boundaries may serve, in turn, as a source for another morphogen gradient that will pattern the neighboring cells. The capacity to translate a gradient to defined borders of gene expression lies at the heart of development.

The translation of graded signals to sharp transcriptional responses has been studied in most detail at the early stages of *Drosophila* embryogenesis. At this phase, the embryo is a syncytium comprised of 5000 nuclei. The anterior–posterior axis is patterned by a concentration gradient of the transcriptional activator Bicoid (Driever and Nusslein-Volhard, 1988), whereas the dorso-ventral axis is patterned by a graded nuclear localization of the transcriptional activator Dorsal (Jiang and Levine, 1993). In both cases, cooperative binding of multiple transcriptional activator molecules is required for activating target-gene expression. This cooperativity seems to generate tight expression boundaries, with the number of binding sites dictating the sharpness of the border and the binding affinity of these sites determining the concentration threshold for gene activation (Driever and Nusslein-Volhard, 1988; Struhl *et al*, 1989; Jiang and Levine, 1993).

In most developmental contexts, morphogens are secreted to the extracellular milieu and act as signaling molecules that activate an intracellular signaling cascade upon binding to their receptors on the cell membrane. Most activated enzymatic cascades culminate in the induction of target-gene expression, but the intracellular signals may be modulated before reaching the nucleus. In particular, several mechanisms were proposed to generate a switch-like response at the signaling level, converting a graded enzymatic activity into a binary decision. For example, when an enzyme independently regulates several sequential reactions, a cooperative response could ensue leading to a sharp threshold. A bi-stable switch also can be generated by reinforcing the response through a positive feedback loop (Ferrell, 2002).

Alternatively, Goldbeter and Koshland have demonstrated that a switch can be generated even at the level of

phosphorylation of a single protein, provided that this phosphorylation is reversible. This mechanism, which they termed zero-order ultrasensitivity, operates when the levels of the two opposing enzymes (kinase and phosphatase) are limiting and the substrate is in excess, such that the rates of both phosphorylation and dephosphorylation reactions become essentially independent of the levels of substrate. In this case, a stable situation will be reached, whereby the protein pool is fully phosphorylated or dephosphorylated (Goldbeter and Koshland, 1981). The capacity of this mechanism to generate thresholds during development was proposed (Goldbeter and Wolpert, 1990), but its applicability to actual developmental patterning processes is yet to be established.

The *Drosophila* embryonic ventral ectoderm is patterned by a graded activation of the epidermal growth factor receptor (EGFR). The principal ligand in this system is the TGF-α homolog Spitz, which is secreted by a single row of midline glial cells at the center of the ventral ectoderm (Golembo *et al*, 1996a). The binding of Spitz to EGFR activates mitogen-activated protein kinase (MAPK), which regulates a battery of target genes by inducing the expression of the ETS-domain transcriptional activator PointedP1 (PntP1) (Gabay *et al*, 1996) and facilitating the degradation of the antagonizing ETS-domain transcriptional repressor Yan (Lai and Rubin, 1992; O'Neill *et al*, 1994).

We wished to dissect the conversion of graded MAPK activation in the ventral ectoderm of the *Drosophila* embryo to sharp response borders. Several features make the system amenable and advantageous for this analysis. First, the activating signal, that is, the secreted ligand Spitz, emanates from a defined source that is restricted to a single row of cells positioned along the midline of the ventral ectoderm (Golembo *et al*, 1996a). Second, the response in the adjacent ectodermal cells can be directly assayed *in situ* by an antibody recognizing activated MAPK (dpERK, the double-phosphorylated form of MAPK) (Gabay *et al*, 1997), and analyzed over the entire ectoderm encompassing dozens of cell rows. This allows for an integrated analysis of multiple individual cells in a single embryo. Third, an antibody that recognizes Yan is available, allowing for a direct *in situ* readout of Yan protein degradation (Rebay and Rubin, 1995). Finally, the crucial components of the system can be manipulated genetically, allowing alterations in the level of activation, elimination or ectopic expression of components.

Here, we ask how Yan degradation boundaries are defined. We demonstrate that cells in which Yan is degraded are confined to a distinct region, whose sharp boundaries are within the graded region of activated MAPK. Using a combination of theoretical and experimental analyses, we present evidence that the tight degradation border of Yan is generated through a zero-order ultrasensitivity-like mechanism (Goldbeter and Koshland, 1981, 1984).

Results

Graded MAPK activation is converted to a sharp border of Yan degradation

To examine if the Yan degradation borders are indeed generated by graded MAPK activity, we compared the patterns of MAPK activation and Yan protein distribution. We previously demonstrated that Spitz is capable of activating MAPK and target-gene expression up to five cell rows from the midline (Golembo *et al*, 1996a; Gabay *et al*, 1997). Using the dpERK antibody, this activation pattern was followed in detail at the onset of EGFR ligand release from the midline (beginning of stage 10). Almost all cells in the ventral-most row on each side of the midline exhibit prominent dpERK staining, whereas in the second and third rows, cells displaying lower or vanishing levels of dpERK are detected. In some regions, moderate dpERK staining expands up to five rows from the midline (Figure 1A and C). Thus, in contrast to some biological systems where MAPK activation itself displays a sharp, switch-like dependence on the external signal (Ferrell, 2002), here MAPK activation displays a graded spatial distribution.

To examine whether the graded MAPK activation is translated into sharp response borders, we followed the distribution of PntP1 and Yan proteins. At stage 10, PntP1 is expressed in 2–3 cell rows on each side of the midline, and exhibits a sharp threshold (Figure 1E). The region of Yan degradation is also narrower and sharper than the profile of dpERK. Yan protein is absent from 1 to 2 cell rows on each side of the midline, whereas the adjacent rows display Yan at high levels that are comparable to the more lateral cells (Figure 1B, D and F). A switch-like response converting a broader activated MAPK pattern to sharp borders of Yan degradation is thus implicated. As the border of Yan degradation is included within the PntP1 expression domain, Pntp1 expression or its target genes are not likely to be instructive for defining the position of this border.

We asked if MAPK activation is necessary and sufficient for the degradation of Yan. *rhomboid*-mutant embryos, in which no EGFR activation takes place, fail to degrade Yan in the ventral ectoderm (Figure 1G). Conversely, induction of EGFR following expression of the active ligand cleaved Spitz (cSpi) by *prd-Gal4* in a seven-stripe pattern perpendicular to the midline leads to the degradation of Yan in the same domains (Figure 1H). Does MAPK activation play an instructive role in determining the border of Yan degradation? In *argos*-mutant embryos, where MAPK activation is expanded by 1–2 cell rows (Golembo *et al*, 1996b; Gabay *et al*, 1997), the border of Yan degradation was similarly shifted (Figure 1I). We conclude that MAPK activation is both essential and sufficient for Yan degradation. Moreover, the level of activated MAPK determines the position of the degradation border.

Activation of MAPK by EGFR in the ventral ectoderm at stage 10 follows an earlier activation of the pathway in the same tissue, prior to gastrulation. Signaling in the first stage is not affected by Argos, and hence only the second phase of MAPK activation is expanded in the absence of Argos, as demonstrated both experimentally and computationally (Gabay *et al*, 1997; Reeves *et al*, 2005). The demonstration that the degradation border of Yan is affected by Argos implies that it is indeed determined at stage 10, when EGFR is activated by the ligand provided by the midline glial cells.

To ascertain that the disappearance of Yan in regions of high MAPK activity results only from post-translational responses, we monitored the distribution of *yan* RNA at the same stage. The expression of *yan* is uniform throughout the ectoderm at

stages 9–11 (Figure 1J). Upon expression of cSpi in a *prd*-stripe pattern, the level of *yan* RNA was even elevated in the regions of ectopic EGFR signaling (Figure 1K). Thus, the absence of Yan protein is not a result of a transcriptional response. We also ruled out a possible feedback of Yan on MAPK activation, by demonstrating that the endogenous patterns of activated MAPK (monitored by dpERK antibodies) were not altered following expression of Yan, or Yan activated (a Yan construct lacking the phosphorylation sites), by *prd-Gal4* (not shown).

Mae is necessary but not instructive in determining Yan degradation border

The SAM domain protein Mae/Edl has been shown to be essential for Yan degradation, by dissociating the Yan polymer and exposing S127 on Yan for MAPK phosphorylation (Baker *et al*, 2001; Tootle *et al*, 2003; Qiao *et al*, 2004). Mae expression in the ventral ectoderm is induced by EGFR signaling (Vivekanand *et al*, 2004) and is mediated by PntP1 (Figure 2B). We wanted to examine if the levels of Mae are significant for establishing the Yan degradation borders.

In *mae* mutants, Yan is stabilized in all cell rows, indicating that Mae is essential for degrading Yan (Figure 2A). To examine if Mae is also instructive in determining the borders of Yan degradation, the levels of Mae were ectopically elevated either by inducing PntP1 expression using the *prd-Gal4* driver, or by inducing *mae* itself using the same driver. In both cases, no alteration in the pattern of Yan degradation was detected (Figure 2C and D). Moreover, we observed that in normal embryos, some of the cells expressing the PntP1 protein and the *mae*-LacZ reporter still retained the Yan protein (Figures 1F and 2E). We conclude that Mae is not the limiting factor in defining Yan degradation, as its expression boundaries are not instructive for establishing the border of Yan degradation.

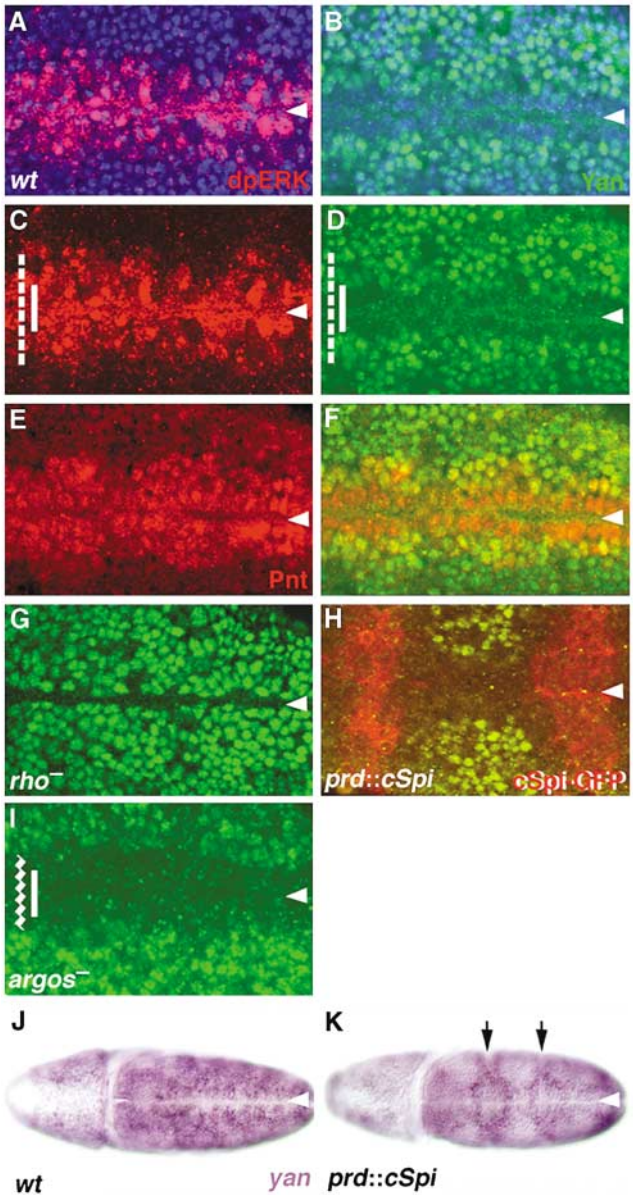

Yan phosphorylation is the critical MAPK-dependent step in Yan degradation

Phosphorylation of Yan by MAPK on serine 127 was shown to be important for targeting Yan to nuclear export and degradation (Qiao *et al*, 2004). To verify that this is indeed the critical MAPK-dependent step, we generated a Yan protein in which this residue was replaced by the phosphomimetic residue aspartic acid (termed Yan^{D}), and expressed it by *prd-Gal4*. The Yan^{D} protein was recognized by the nuclear export machinery, as it was degraded in the ventral-most cells

Figure 1 Graded MAPK activation in the ventral ectoderm is instructive to establish a sharp border of Yan degradation. (**A, C**) Wild-type embryo at stage 10 shows graded activation of MAPK that is detected with dpERK antibodies (red). Cell nuclei are monitored by DAPI staining (blue). The activating ligand, Spitz, emanates from the midline glial cells (arrowhead) to trigger EGFR in the adjacent cells. The activation pattern extends up to five cell rows on each side of the midline. At these initial stages of activation, the pattern is fluctuating. More cells showing higher levels of activation are detected close to the midline, but not all cells in the ventral-most row are activated. In a given row, not all the cells display the same level of activated MAPK, whereas the expression of target genes is uniform. We believe that the pattern of activated MAPK is dynamic and fluctuating, while the transcriptional responses result from summation of MAPK activity over time, and are thus more uniform. (**B, D**) Within the domain of MAPK activation, the degradation pattern of Yan (green) at the same stage shows a much more restricted and sharp response. Yan is absent from the first 1–2 ventral-most cell rows and is present at similar levels in all other cell rows. Thus, a mechanism to convert graded MAPK activation to a sharp border of Yan degradation should be operating. The dashed line denotes dpERK borders, whereas the nested solid line represents Yan degradation boundaries. (**E, F**) The borders of PntP1 expression and Yan degradation were monitored in wild-type embryos at stage 10. Expression of PntP1 (red) is broader than the degradation of Yan (green). (**G**) In *rho*-mutant embryos, where EGFR signaling is abolished, no degradation of Yan takes place. (**H**) Ectopic expression of the EGFR ligand, cSpitz-GFP (red), by *prd-Gal4* led to the degradation of Yan in the corresponding domain. EGFR activation is thus necessary and sufficient for Yan degradation. (**I**) An *argos*-mutant embryo, in which normal EGFR activation is enhanced, shows an expansion of the degradation border by 1–2 rows on each side (waved line versus solid line). Thus, the level of MAPK activation is instructive for positioning the Yan degradation border. (**J**) At stage 10, *yan* RNA shows a uniform distribution, indicating that the basis for the disappearance of Yan is only post-transcriptional. (**K**) Ectopic activation of EGFR enhances the expression level of *yan* (arrows). The embryo was understained compared to panel J, to allow detection of the elevated *yan* levels.

(Figure 2F). It is also functional, as monitored by the capacity of high levels of Yan^D to repress transcription of *mae* (not shown). In the lateral regions, which do not express Mae, Yan^D was not degraded (Figure 2G).

We examined the degradation border of Yan^D following coexpression with Mae. A significant portion of the cells within the *prd* stripes displayed complete degradation of Yan^D, such that the levels of expression were analogous to those seen in cells outside the *prd* stripes expressing only endogenous Yan. The remaining cells within the stripes retained Yan^D in their nuclei, giving rise to a 'salt and pepper' pattern within the *prd* stripe (Figure 2H). We do not know why some of the cells were unable to cope with the nuclear export of Yan^D. However, the ability of most cells to degrade Yan^D in the absence of MAPK activity is consistent with Yan phosphorylation being the limiting MAPK-dependent step in defining Yan degradation borders. Yan^D was also coexpressed with PntP1. Indeed, the Yan^D protein disappeared from most nuclei within the *prd* stripes, giving rise to a pattern that resembled the distribution of endogenous Yan (Figure 2I and J). The more efficient nuclear export and degradation of Yan^D under these conditions may be explained by the induction of additional PntP1 targets that facilitate Yan^D degradation in a MAPK-independent manner.

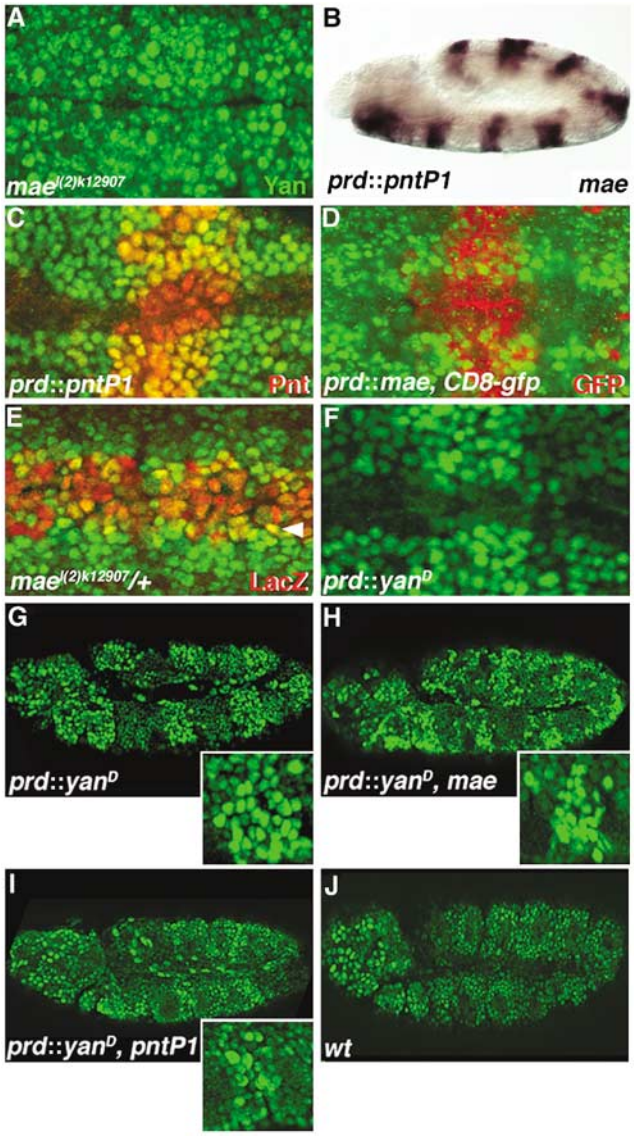

Mathematical modeling of the Yan degradation network

The above results confine the mechanism translating graded MAPK activation into sharp degradation borders to the Yan phosphorylation circuitry. To try and infer the underlying mechanism, we analyzed this circuitry using mathematical modeling.

Although S127 appears to be the critical residue, Yan can be potentially phosphorylated on seven additional sites (Rebay and Rubin, 1995), and it is formally possible that multiple, subsequent bindings of MAPK to Yan facilitate Yan degradation. We thus considered the number of phosphorylation events as a free parameter, n. We also assumed that Yan phosphorylation is reversible, and that dephosphorylation is catalyzed by a phosphatase P. As phosphorylated Yan that is exported from the nucleus is degraded (Tootle *et al*, 2003), we assigned phosphorylated Yan a degradation rate (λ_p) that is higher than that of the non-phosphorylated form (λ). Finally, we assumed that Yan is continuously produced at a fixed rate.

Taking these considerations into account, we modeled the system using the following set of differential equations and two enzyme conservation equations:

$$(1)\ \frac{dY}{dt} = -a_m Y[MAPK_f^*]^n + d_m[Y\,MAPK^*] + k_p[Y_pP] + \alpha - \lambda Y$$

$$(2)\ \frac{d[Y\,MAPK^*]}{dt} = a_m Y[MAPK_f^*]^n - (d_m + k_m)[Y\,MAPK^*]$$

Figure 2 Yan degradation requires activated MAPK and Mae, but the degradation border does not depend on endogenous Mae levels. (**A**) In *mae*-mutant embryos, homozygous for the *mae*$^{l(2)k12907}$ null allele, no degradation of Yan was detected, indicating that Mae is essential for degradation. (**B**) Expression of PntP1 by *prd-Gal4* induces the corresponding expression of *mae*. (**C, D**) To ask if the border of Yan degradation is dictated by the endogenous levels of Mae, the distribution of Yan was monitored following elevation of Mae levels. When *prd-Gal4* was used to drive expression of PntP1 (which induces expression of endogenous *mae*) or Mae itself, no alterations in the degradation border of Yan were observed. This indicates that Mae is not instructive for the position of the border. Expression of *UAS-mae* was monitored by the expression of *UAS-CD8-gfp*, which was recombined to the same chromosome. (**E**) The borders of *mae* expression and Yan degradation were monitored in wild-type embryos at stage 10. Expression of *mae* (marked by *lacZ* expression—red) is broader than the degradation of Yan (green). The presence of cells expressing both Yan and *mae* (arrowhead—yellow) indicates that in spite of the presence of Mae, Yan was not degraded in these cells. (**F**) Expression of Yan^D by *prd-Gal4* leads to degradation of the protein in the ventral-most cell rows, similar to endogenous Yan. (**G**) In the lateral regions, Yan^D was not degraded. (**H**) To separate between the requirement for MAPK and Mae in Yan^D degradation, Yan^D was coexpressed with Mae, leading to degradation of Yan^D in lateral cells. Not all cells within the *prd* stripe degraded Yan^D for unknown reasons, giving rise to a 'salt and pepper' pattern. (**I**) Yan^D was also coexpressed with PntP1, giving rise to degradation of Yan^D in most cells within the *prd* stripe. (**J**) Similar view of a *wt* embryo, displaying the endogenous Yan pattern. Insets in panels G–I show the second anterior *prd* stripe.

$$(3)\ \frac{dY_p}{dt} = -a_p Y_p[P_f] + d_p[Y_pP] + k_m[Y\,MAPK^*] - \lambda_p Y_p$$

$$(4)\ \frac{d[Y_pP]}{dt} = a_p Y_p[P_f] - (d_p + k_p)[Y_pP]$$

$$(5)\ [MAPK^*] = n[Y\,MAPK^*] + [MAPK_f^*]$$

$$(6)\ [P] = [Y_pP] + [P_f]$$

Here, $[MAPK_f^*]$ and $[P_f]$ denote the concentrations of free activated MAPK and the free phosphatase P, respectively. $[Y\,MAPK^*]$ and $[Y_pP]$ denote the concentration of activated MAPK and the phosphatase at their complex form. The input to this model is the level of activated MAPK, whereas its output is the total level of Yan, $Y^{tot}=Y+Y_p$. As activated MAPK is spatially graded, tight degradation borders are achieved when Y^{tot} displays a switch-like dependency on the level of activated MAPK.

The model (equations (1)–(6)) is general and can accommodate several molecular mechanisms, depending on the values of the associated rate constants and enzymatic concentrations. To try and identify the mechanism used for translating the activated MAPK signal to Yan degradation, the behavior of the system was examined at four different limits. First, the non-cooperative, linear model was considered, where we assume that a single phosphorylation of Yan by MAPK is required (n=1), and that the corresponding enzymatic reactions are first order (i.e. enzymes are in excess and bind most of the Yan molecules). Second, the cooperative, linear model with $n>1$ was examined. Third, we consider the non-cooperative, zero-order case, with n=1 and reactions that function at the zero-order regime (i.e. enzymes are present at limiting amounts so that most Yan is free and $Y^{tot} \gg K_m, K_p$).

Finally, positive feedback is an additional prominent mechanism that can generate a switch-like response. Although no such feedback was identified in this system yet, it is formally possible that the presence of Yan in its phosphorylated form functions to enhance Yan degradation (e.g. by repressing the activity of the phosphatase). To account for this possibility, we extended the model to allow for an arbitrary dependence of the rate constants on Yan, or Yan-p levels. As a specific feedback mechanism, we assumed that Yan dephosphorylation rate decreases monotonically with Yan-p level, with $k_p \rightarrow k_p[K_f^l/(K_f^l + Y_p^l)]$, where K_f is constant and l is the feedback degree of nonlinearity. Importantly, our qualitative results below do not depend on this specific implementation (Supplementary information). Thus, as a fourth limiting case, we considered a feedback system with single phosphorylation sites (n=1) and enzymatic reactions that function at the first order.

We solved for the steady-state levels of Yan defined by the four cases described above, assuming a graded distribution of MAPK (see Materials and methods). The results are summarized in Figure 3. As expected, the first-order, non-cooperative model generated a relatively smooth spatial gradient of Yan degradation. Indeed, when the reaction rate depends linearly on the level of enzyme as well as on the level of substrate, any alteration in enzyme level is compensated by a reciprocal change in substrate level. In contrast, a clear switch-like behavior is observed for the three other cases.

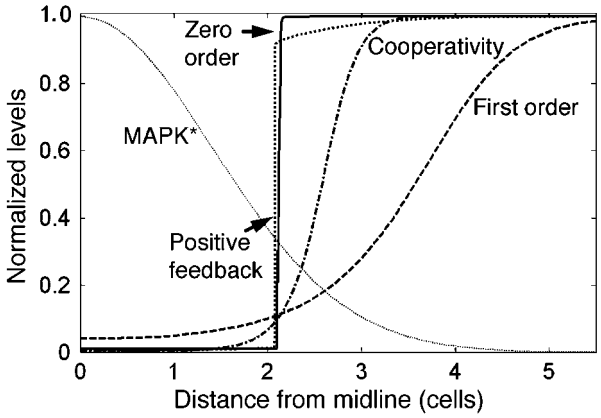

Figure 3 Different mechanisms could generate a sharp threshold of Yan degradation. Yan steady-state concentration was found by numerical simulations (see Materials and methods for further information). The concentration levels are normalized with the corresponding maximal concentrations. At first order, the graded reduction in active MAPK distribution (thin dotted line) leads to a smooth gradual increase in the level of total Yan concentration (dashed line). In contrast, a clear switch-like behavior is observed for the three other cases, namely the cooperative, linear model (dash/dot line), the feedback model (dotted line) and the zero-order model (solid line).

Thus, it appears that cooperativity, positive feedback and zero-order ultrasensitivity could all account for the sharp borders of Yan degradation. Moreover, although the non-cooperative, linear case generates a much smoother dependence of Yan degradation on MAPK activity, it is hard to rule out this mechanism, as additional averaging is probably carried out at the levels of individual cells, and it may be that our experimental resolution of Yan detection is too low to distinguish a sharp, switch-like response from a smoother, first-order dependence.

Distinguishing between the different models of Yan degradation

As the wild-type situation does not allow to differentiate between the possible threshold mechanisms, we studied computationally the response of the system to overexpression of Yan. Specifically, we examined the possible perturbation to the steady-state Yan distribution (Figure 4), and the time to reach this steady state, upon increasing the levels of Yan production (Figure 5).

Within the non-cooperative, linear model, the steady-state Yan distribution is highly sensitive to the total level of Yan, such that increasing the level of total Yan leads to a shift in the degradation boundaries toward the source of MAPK activity (Figure 4A and E). Similar strong dependence is seen also in the feedback system (Figure 4C and E). In fact, it can be shown analytically that when the enzymatic reaction is at first order, the sensitivity of the switch threshold to changes in Yan levels will be at least linear, independently of possible feedbacks (Supplementary information). In sharp contrast, in both the cooperative and the zero-order models, the position of the

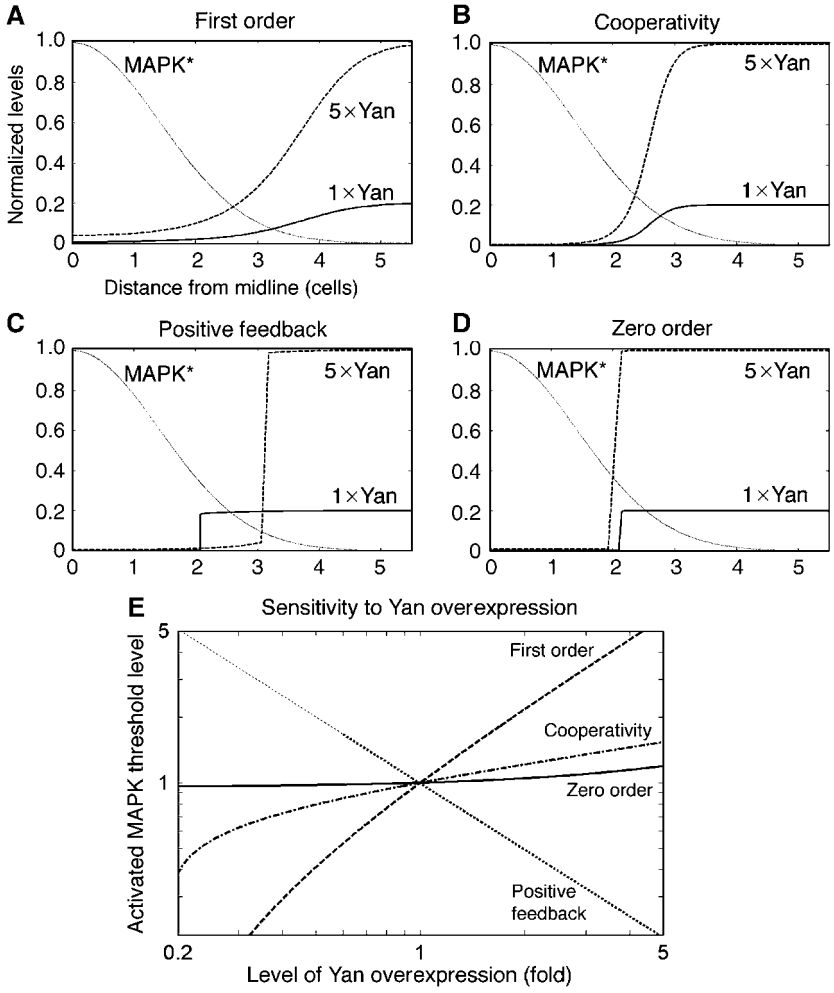

Figure 4 Computational predictions of the steady-state Yan degradation pattern upon its overexpression. (A–D) The steady-state profiles of Yan for different levels of Yan protein for some reference level (× 1) of Yan production rate and for a five-fold (× 5) increase in this production rate. Yan levels are normalized by the initial level of the overexpressed network. The expected distributions are calculated for the first-order, non-cooperative model (**A**), first-order, cooperative model (**B**), first-order model with positive feedback (**C**) and zero-order model (**D**). Note that an increase in Yan levels in the linear, non-cooperative case and in the linear positive feedback case significantly alters the threshold positions of Yan degradation. In sharp contrast, threshold positions are insensitive to the level of Yan production in both the first-order, cooperative model and the zero-order model. (**E**) The critical MAPK value was examined for different levels of Yan overexpression. The critical MAPK value is defined as the level of MAPK activity for which the absolute Yan level reaches a certain threshold. We defined the threshold as 90% of the maximal level of the most underexpressed situation for Yan (chosen here as 0.2 of the endogenous Yan level). All curves are normalized such that the critical MAPK value equals one for the wild type (overexpression of one-fold). As can be seen, the critical MAPK value is highly sensitive to Yan overexpression in the non-cooperative, linear cases, either in the absence (dashed line) or presence of a positive feedback loop (dotted line). For the positive feedback case, the critical MAPK value is shown for overexpression values larger than 0.6, because for lower values the network exhibits an abnormal behavior (Supplementary information). In contrast to the non-cooperative linear models, the cooperative first-order case is considerably less sensitive (dash/dot line). Similarly, the critical MAPK level hardly changes in the zero-order case (solid line). Simulations were obtained by solving equations (1)–(6) numerically. See Materials and methods for the rate constants used.

switch in Yan degradation does not depend on the total Yan level (Figure 4B, D and E).

The temporal convergence to steady state further differentiates between the zero-order and linear models. In the case of first-order kinetics, where the substrate is limiting and the enzyme is in relative excess, Yan degradation is exponential, with a time constant that is independent of substrate level. Increasing Yan levels will not have an effect on the time required to reach steady state (Figure 5A, B and E). In the case of positive feedback, an increase in Yan level results in a minor increase of Yan degradation time (Figure 5C and E). In sharp contrast, in the case of zero-order kinetics, Yan degradation is linear, rather than exponential in time. Accordingly, the time to reach steady state will increase approximately linearly with the level of substrate (Figure 5D and E). Thus, a central prediction of zero-order kinetics is that upon overexpression of Yan, the position of the threshold for Yan degradation will not be altered, but the time to reach steady state will be significantly longer, such that intermediate states could be captured.

Yan degradation pattern fits zero-order predictions

To examine experimentally the kinetics of Yan degradation, we expressed Yan ectopically using the *prd-Gal4* driver. When a Yan construct that cannot be phosphorylated was expressed, it was maintained in the *prd* stripes, indicating that

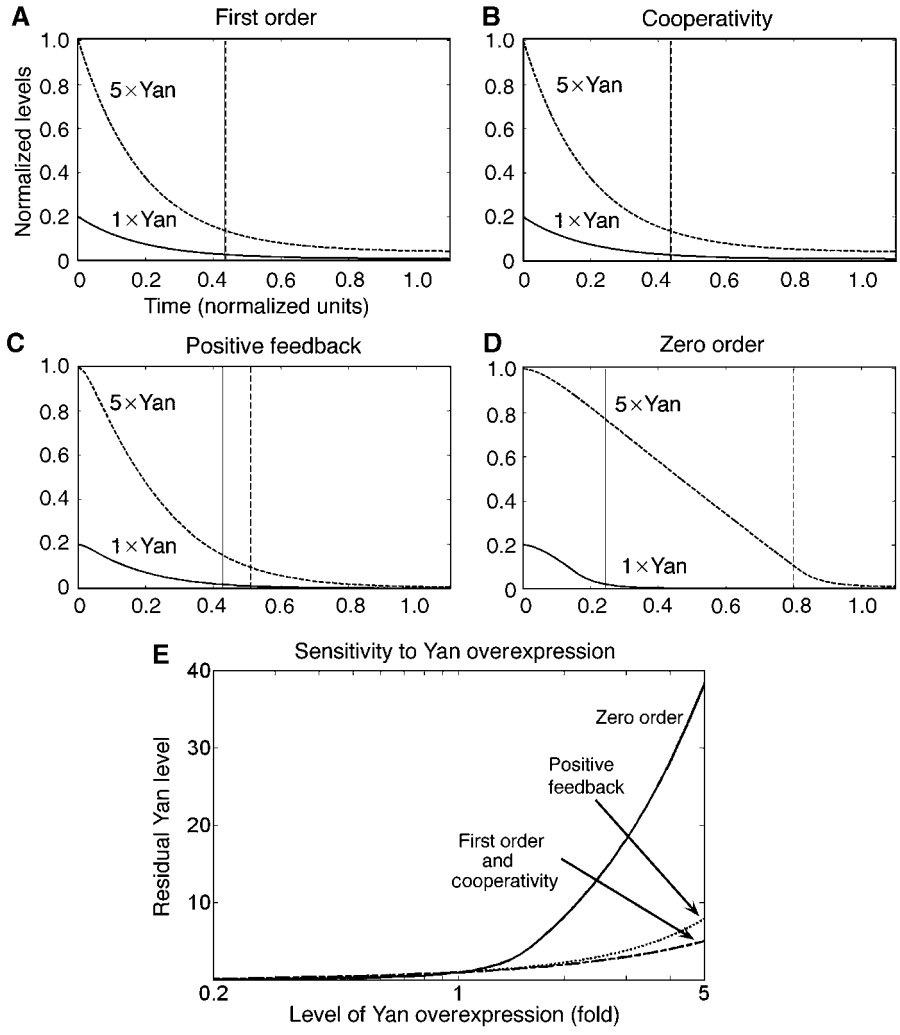

Figure 5 Temporal convergence to steady state upon Yan overexpression. (A–D) Yan dynamics for different levels of Yan protein for some reference level (× 1) of Yan production rate and for a five-fold (× 5) increase in this production rate. Yan levels are normalized by the initial level of the overexpressed network. The kinetics of Yan degradation is measured immediately adjacent to the midline, a position where most Yan is degraded at steady state. The expected distributions are calculated for the first-order, non-cooperative model (**A**), first-order, cooperative model (**B**), first order with positive feedback model (**C**) and zero-order model (**D**). The vertical bars (solid line for × 1 Yan and dashed line for × 5 Yan) indicate the time when 90% of Yan was degraded. Note that in both the linear, non-cooperative case and the linear, cooperative case, degradation time is relatively independent of the increase in Yan levels. In the positive feedback case, an increase in Yan level results in a minor increase of the degradation time. When kinetics is zero order, the degradation time strongly depends on Yan levels. (**E**) Sensitivity of absolute Yan level dynamics to overexpression. The residual Yan level is defined as the absolute level of Yan left in the overexpressed network, calculated at the time when Yan in the wild-type network (× 1) reaches 5% of its maximal value. For each model, the residual Yan level was examined for different levels of Yan overexpression. All curves are normalized such that the residual Yan value equals one for the wild type (overexpression of one-fold). As can be seen, the temporal decay of Yan at zero-order kinetics (solid line) is highly sensitive to Yan overexpression, whereas all first-order models display only a moderate sensitivity (non-cooperative—dashed line, cooperative—dash/dot line and positive feedback—dotted line). Simulations were obtained by solving equations (1)–(6) numerically. See Materials and methods for the rate constants used.

phosphorylation is essential for Yan export and degradation (Figure 6A). In contrast, a dynamic pattern was observed when *wt* Yan was expressed by the same driver. At stage 9, prior to activation of MAPK, both endogenous and ectopic Yan protein were detected throughout the ventral ectoderm (Figure 6B). Judging by the intensity of Yan antibody staining, the level of ectopic Yan is 5- to 10-fold higher than the level of endogenous Yan.

Graded MAPK activation is induced at the onset of stage 10. Monitoring Yan at this stage, we found that endogenous Yan disappeared. In contrast, exogenous Yan was still detected in all cells where it was induced (Figure 6C and D), and was degraded in the ventral-most cells only in older embryos. In these older embryos, the boundaries of degradation of both exogenous and endogenous Yan were perfectly aligned (Figure 6E and F). Thus, the position of the steady-state Yan borders is insensitive to the total Yan levels. This result is consistent with the linear, cooperative model and with the zero-order, ultrasensitivity mechanism, but rules out the possibility of a positive feedback as generating the switch (Figure 4).

To further differentiate between the cooperative and zero-order model, we examined in detail the intermediate stage, where endogenous Yan has disappeared whereas the exogenous protein was still present. In an embryo collection of

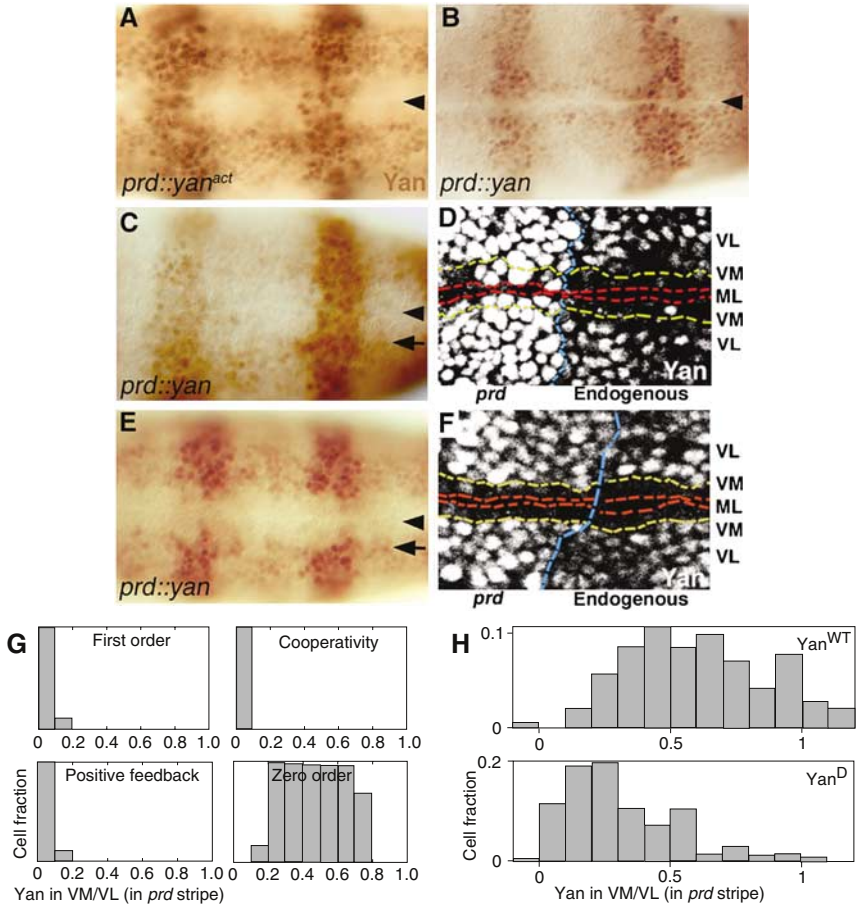

Figure 6 Experimental validation of zero-order kinetics of Yan degradation. *prd-Gal4* was used to drive Yan expression in stripes. (**A**) Yan construct that cannot undergo phosphorylation is maintained in the *prd* stripes. A stage 11 embryo is shown. (B–F) Expression of a *wt* Yan construct. (**B**) At stage 9, endogenous and ectopic Yan proteins are detected and extend to the ventral midline (arrowhead), as EGFR/MAPK activation has not ensued. (**C, D**) An intermediate pattern is detected at stage 10 in a significant portion of embryos, where endogenous Yan in the ventral-most rows has already disappeared (arrow), whereas ectopic Yan was unaltered. The midline (ML) is marked by a dashed red line, the border of Yan degradation between the ventral-most (VM) and ventro-lateral (VL) cells by a dashed yellow line and the border of the ectopic *prd* stripe by a dashed blue line. (**E, F**) In late stage 10 embryos, ectopic Yan was also degraded in the ventral ectoderm, and the degradation border is aligned with the endogenous one (arrow). The detection of an intermediate step implying longer degradation times for ectopic Yan, as well as the alignment of degradation borders for endogenous and ectopic Yan, validates the zero-order kinetics of Yan degradation. (**G**) Prediction of the distribution of ectopic Yan intensities within individual nuclei after completion of degradation of endogenous Yan, according to the four models. In the three first-order cases, the rate of degradation of ectopic Yan is elevated, such that endogenous and ectopic Yan are degraded at comparable times. Thus, at the time when endogenous Yan is degraded, most nuclei are predicted to display ectopic Yan levels that are centered on 0–0.1. Conversely, owing to the linear decay of Yan in the zero-order case, ectopic Yan levels are predicted to be broadly distributed between all values. The abscissa corresponds to the ratio between level of Yan in a given nucleus and the average level of ectopic Yan outside the degradation zone. The ordinate is the fraction of cells displaying each of the values. (**H**) To measure the distribution of ectopic Yan intensities, fluorescent staining in individual nuclei was quantitated. In the embryo shown in panel D, endogenous Yan is degraded in the VM cells (marked by dashed yellow line), whereas ectopic Yan in the same domain is still detectable. The level of Yan in the degradation zone within the *prd* domain in each nucleus was divided by the mean level of ectopic Yan outside this zone, within the same stripe. Plotting the level of ectopic Yan in the degradation zone in individual nuclei gave a distribution that is consistent with the zero-order model (upper panel). The distribution of values across the entire spectrum is indicative of a linear kinetics of degradation. Plotting the level of ectopic Yan^D in individual nuclei within the degradation zone shifted the values to the low levels, indicative of rapid degradation (lower panel). Owing to fluctuations between nuclei in the expression levels of ectopic Yan or Yan^D, some nuclei in the degradation zone gave a value larger than the mean outside the zone and some showed values below the mean for endogenous Yan within the zone. Values above 1.2 and below −0.1 are not shown (15% of the nuclei for Yan and 3% of the nuclei for Yan^D).

100 min encompassing stages 9–11, 38% of the embryos displayed the intermediate pattern (n=55), giving a rough estimate of 38 min to the time required to degrade ectopic Yan. As we cannot follow the kinetics of degradation in live embryos, we reasoned that the kinetic parameters will be reflected by the distribution of intensities of Yan staining within the degradation borders, as compared to the intensity outside the degradation zone. Assuming that endogenous Yan was reduced by at least 95% at the time of observation (our minimal detection), and that the initial levels of exogenous Yan were about five-fold higher than the endogenous (a lower bound derived from early staining), we generated the predicted distribution of intensities for the four models (Figure 6G). Indeed, the distributions are clearly different: the three linear models predict a distribution that is strongly peaked at 0–0.1 intensity of the initial ectopic Yan level, owing to the fact that the elevated levels of Yan gave rise to a higher rate of degradation, such that endogenous and ectopic Yan disappear at comparable times. Conversely, the distribution corresponding to the zero-order ultrasensitivity case is broad

and approximately uniform across a wide range of intensity values, reflecting not only a longer decay time of ectopic Yan levels, but also the linear kinetics of this decay.

To see which of the distributions describes more closely the pattern of exogenous Yan degradation, we designed a Matlab-based image analysis software for semi-automatic analysis of Yan intensities (Figure 6D; Materials and methods). Yan levels were monitored by immunofluorescence, at an intensity that maintained the linear response. Using this program, the ratio between ectopic Yan level in the cells within Yan degradation border and the mean level of ectopic Yan in cells outside this border was measured. Clearly, the distribution of exogenous Yan intensities most closely resembles the prediction of the zero-order ultrasensitivity model (Figure 6H, upper panel).

We note that although there are two consecutive reactions leading to Yan degradation, that is, MAPK-dependent phosphorylation and nuclear export, it is unlikely that nuclear export will function at the zero-order regime and produce the observed behavior. Yan nuclear export utilizes the general CRM1-mediated machinery (Tootle *et al*, 2003), which is ubiquitously utilized for a broad range of proteins (Gorlich and Kutay, 1999), and its components are thought to be in excess. Indeed, when the same methodology was used to follow the level of ectopically expressed Yan^D within the endogenous degradation domain, very few cells with intermediate or high levels of Yan^D were scored (Figure 6H, lower panel), indicating that the kinetics of Yan^D degradation is rapid, as the step of phosphorylation by MAPK was bypassed.

Discussion

Our results established the instructive role of MAPK in defining the border of Yan degradation, and have shown that phosphorylation of S127 by MAPK is the critical event leading to Yan degradation. We thus sought a mechanism that may account for the sharp degradation boundaries of Yan in the embryo, which is generated by the circuitry controlling Yan phosphorylation. The Yan nuclear export pathway has been studied in detail in cell culture (O'Neill *et al*, 1994; Tootle *et al*, 2003; Song *et al*, 2005). These studies indicate that Yan is maintained in the nucleus as a polymer. Association with Mae dissociates the polymer to generate heterodimers that are susceptible for MAPK phosphorylation. Prior to phosphorylation, the association of Yan monomers with the Crm1 nuclear export machinery is low and is further compromised by association with Mae. Following phosphorylation, association of Yan with Crm1 is favored over its association with Mae, and hence nuclear export ensues. Although it was possible in cell culture to induce nuclear export of monomeric Yan in the absence of phosphorylation under conditions where Crm1 is provided in excess, clearly these conditions do not reflect the *in vivo* setting, where Crm1 levels are uniform, and MAPK phosphorlation is essential and instructive for nuclear export. Our studies focus on the dissection of the pathway *in vivo*.

The results have ruled out cooperativity as a source for threshold in this system. Indeed, this model was also regarded as less plausible in view of previous experimental results: although Yan contains eight potential phosphorylation sites, only one of these sites, that is adjacent to the SAM domain (S127), is necessary for Yan nuclear export and degradation (Rebay and Rubin, 1995; Qiao *et al*, 2004).

Zero-order ultrasensitivity emerged as an alternative attractive paradigm. Graded MAPK-dependent activation leading to Yan phosphorylation on the one hand, and a constant rate of Yan dephosphorylation on the other, may generate zero-order kinetics. The motivation to distinguish between the first- and zero-order cases stems from the classic work of Goldbeter and Koshland (1981), who demonstrated that a loop of reversible phosphorylation can function as a threshold generator, through a mechanism they termed 'zero-order ultrasensitivity'. This mechanism is realized when the enzymes are limiting and the substrate is present at levels that significantly exceed the reaction dissociation constants (K_m and K_p), such that both the kinase and the phosphatase are saturated by their substrates. Under these conditions, the rate of the enzymatic reactions is independent of the level of the substrate, and proceeds at maximal speed. The faster reaction will dominate, resulting in a steady-state situation where the substrate is either fully phosphorylated or fully dephosphorylated. Indeed, in such a case, an 'all to none' change in the phosphorylated state of Yan will be observed at a particular value of MAPK activity.

As phosphorylation of Yan by active MAPK is a central component in the Yan degradation network, we reasoned that a zero-order ultrasensitivity-like mechanism may account for the sharp border of Yan degradation. The present system, however, differs from the general ultrasensitivity model in several respects. Foremost, in the general model, the substrate concentration is assumed to be constant, whereas in the present case, Yan production and differential degradation are crucial. In addition, the output in the general model is considered to be the level of the modified substrate, whereas here, the output is the total amount of Yan, as the phosphorylated isoform is targeted to degradation (Figure 7). Despite these differences, we found that a zero-order ultrasensitivity-like threshold mechanism is realized.

The paradigm of zero-order ultrasensitivity has several major advantages for patterning. First, as the border that is generated relies only on the difference between the rates of the two opposing reactions, even small differences in signaling can be converted to a sharp border. Furthermore, it is possible to generate multiple thresholds that rely on the same gradient of enzymatic activity, simply by changing the association constant of one of the two opposing reactions toward different substrates (Goldbeter and Wolpert, 1990). It is important to note that while the gradient of MAPK activation is buffered by feedback loops (e.g. *argos* induction), the opposing Yan dephosphorylation reaction should also be maintained at a fixed rate, to assure a reproducible definition of the border. Finally, as a large pool of molecules is shuttled between two states, minor temporal fluctuations in signaling are buffered by the excess of molecules in the pool. This temporal averaging appears to be particularly valuable in the case of the ventral ectoderm, because the initial MAPK profile is fluctuating and unstable, displaying a 'salt and pepper' pattern of activation. In contrast, the resulting Yan degradation profile is highly ordered and stable.

The Yan overexpression experiment provides also a rough estimate of the time required to degrade endogenous Yan

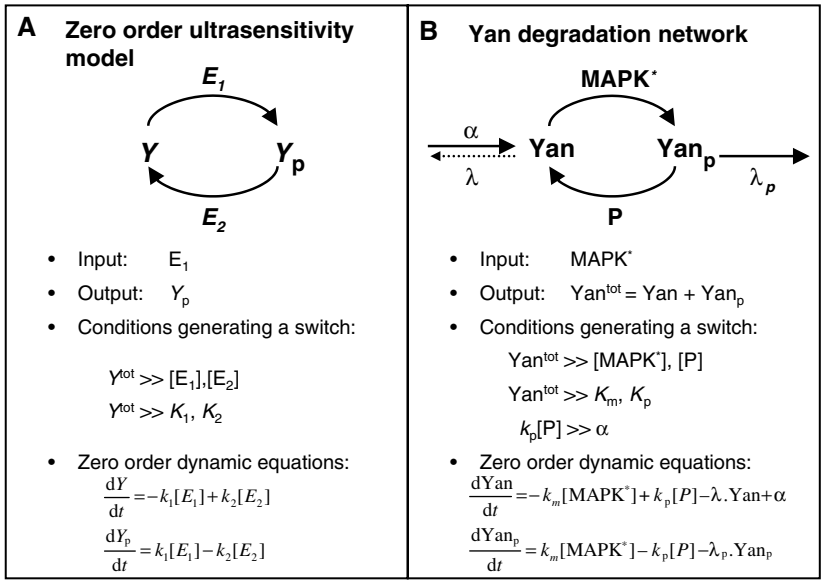

Figure 7 Yan degradation network versus the classical zero-order ultrasensitivity model. In contrast to the classical model, Yan degradation network does not assume a constant concentration of total Yan. Rather, Yan is produced at a fixed rate α. Yan degradation rates of the non-phosphorylated and phosphorylated isoforms (λ and λ_p) were chosen such that $\lambda_p \gg \lambda$, since phosphorylated Yan that is exported from the nucleus is degraded. The low degradation values of non-phosphorylated Yan may be realized by mechanisms including, for example, the Crm1-dependent nuclear export of the non-phosphorylated Yan monomer. Conversely, the possible repression of nuclear export of phosphorylated Yan by binding to Mae may help to maintain its pool at a level that is sufficiently high (above the K_m for the phosphatase) to allow a zero-order regime (Song *et al*, 2005). In both cases, the input of the network is the total concentration of activated kinase (E1 or MAPK). The output of Yan degradation network is the total amount of Yan. Similar to the classical model, a switch-like behavior is generated when the substrate is in excess with respect to the dissociation constants for the two opposing enzymes. Zero-order dynamic equations are derived using quasi-steady-state assumptions and zero-order conditions.

protein in response to MAPK activation. The time required to degrade exogenous Yan was ~40 min, and the ectopic Yan levels were five-fold higher than the endogenous levels (according to Matlab quantification; see Materials and methods). Thus, the endogenous Yan is likely to be degraded within a few minutes. This period is negligible with respect to the time window of 1–2 h in which patterning of the ventral ectoderm by EGFR takes place, whereas it may be sufficiently long in order to buffer local fluctuations in MAPK activation.

In conclusion, this study establishes the application of a zero-order ultrasensitivity mechanism for translating a graded signal into sharp response borders during developmental patterning. This mechanism may be used not only to define borders of protein degradation, but also to determine transcription boundaries, through reversible phosphorylation leading to activation of transcription factors.

Materials and methods

Constructs, fly lines and staining procedures

The UAS-*mae* construct was generated by inserting the full-length cDNA (obtained from D Baker) into the *Eco*RI site of pUAST, and transgenic flies were generated. Yan^D was generated by using the oligonucleotide GTGGCACCTGCCTAATGATCCAGTGACGCCCAC and its complementary oligonucleotide, and the QuickChange II XL site-directed mutagenesis kit by Stratagene, to mutate codon 127 of the *yan* cDNA (obtained from I Rebay) in Bluescript. The mutated gene was inserted into pUAST and used to generate transgenic lines. An insertion on the second chromosome was used for overexpression, either alone or following recombination with *UAS-mae*. An insertion on the third chromosome was used for recombination with *UAS-PntP1*. Other lines used include flies containing *UAS-cSpi-GFP*, *UAS-pntP1* (obtained from C Klambt), *UAS-yan*, *UAS-yan activated* (obtained from I Rebay), *UAS-CD8-gfp* and *prd-Gal4*. Mutant lines include *argos*$^{delta\ 7}$, *rhomboid*$^{delta\ 38}$ and *mae*$^{l(2)k12907}$ (representing an enhancer trap in *mae*, obtained from D Baker).

Antibodies used include mouse anti-dpERK (Sigma), mouse anti-Yan (obtained from I Rebay) and rabbit anti-PntP1 (obtained from J Skeath). For anti-dpERK staining of embryos, fixation was carried out in 8% formaldehyde/PBS and 50 mM EGTA for 25 min, primary antibody incubated for 2 h at room temperature (RT) in 0.1% Tween/PBS and secondary antibody (goat anti-mouse biotin; Chemicon) incubated for 60 min at RT. It was amplified by streptavidin-HRP for 30 min at RT, followed by incubation with tyramide biotin for 20 min (both from Perkin Elmer TSA biotin system). Finally, embryos were incubated with streptavidin-Cy3 for 30 min at RT (Jackson ImmunoResearch). For Yan immunofluorescence, all incubations and washes were carried out with 0.1% saponin in PBS. Following tyramide amplification, embryos were incubated with streptavidin-Cy2 for 30 min at RT (Jackson ImmunoResearch). For *in situ* hybridization, a probe was prepared using T7 RNA polymerase and the Roche RNA DIG labeling mix. Fixation, hybridization and detection were according to http://www.biology.ucsd.edu/~davek/.

Mathematical modeling

Simulation results (Figures 3–5 and 6G) were obtained by solving numerically equations (1)–(4) using MATLAB ODE15s function. Graded distribution of active MAPK was assumed, according to $[MAPK^*] \propto \exp(-d^2/4)\mu M$, where d is the distance from the midline in units of cells. Other graded distributions of MAPK* (e.g. exponential) were analyzed and gave rise to Yan profiles that were similar to those obtained according to the Gaussian MAPK* distribution (not shown). We present the analyses based on the exponential MAPK* distribution. The following parameters were used: for the non-cooperative, first-order case, $\alpha = 10^{-2}\,\mu M\,s^{-1}$, $\lambda = 5\times10^{-4}\,s^{-1}$, $\lambda_p = 1\,s^{-1}$, $K_m = 500\,\mu M$, $K_p = 500\,\mu M$, $k_p[P] = 10\,\mu M\,s^{-1}$ and $k_m = 1\,s^{-1}$. Here, k_m and k_p are the rates of phosphorylation and dephosphorylation from the complex form, respectively, and $(K_m)^n \equiv (d_m + k_m)/a_m$ and $K_p \equiv (d_p + k_p)/a_p$ are the reaction dissociation constants. For the cooperative, first-order case, $n=4$, $\alpha = 10^{-2}\,\mu M\,s^{-1}$, $\lambda = 5\times10^{-4}\,s^{-1}$, $\lambda_p = 1\,s^{-1}$,

k_m=15.625 × 10^6 s^{-1}, d_m=15.625 × 10^6 s^{-1}, a_m=5 × 10^{-4} μM^{-n} s^{-1}, K_p=500 μM and k_p[P]=10 μM s^{-1}. Note that K_m=500 μM, as in the non-cooperative case. For the first-order positive feedback case, α=3.5 × 10^{-3} μM s^{-1}, λ=5 × 10^{-5} s^{-1}, λ_p=0.1 s^{-1}, K_m=500 μM, K_p=500 μM, k_p[P]=5 × 10^4 μM s^{-1}, k_m=1 s^{-1}, K_f=4 × 10^{-3} μM and l=5. For the zero-order case, α=10^{-2} μM s^{-1}, λ=10^{-5} s^{-1}, λ_p=10^{-3} s^{-1}, K_m=10^{-3} μM, K_p=10^{-3} μM, k_p[P]=0.2 μM s^{-1} and k_m=0.1 s^{-1}. Note that different parameters were used for the four models, to ensure a similar dynamic range. Our qualitative results do not depend on those choices. To simulate Yan overexpression, we increased its production rate (α) by a factor of 5 (Figures 4A–D, 5A–D and 6D). The dynamics of each model (Figure 5A–D) was solved at the midline, assuming maximal initial Yan level: Y=α/λ, Y_p=0. For Figures 4E and 5E, we changed the production rate from 1/5 to 5 times the wild type. The results in Figure 4E were fitted to curves using the Matlab Fit function with minimal confidence of 99% (estimated using the Matlab Fit function adjusted R^2 parameter). First- and zero-order were fit to a linear line, the cooperative case to $f(x) = a + b \cdot |x - x_0|^{\frac{1}{n}}$ and positive feedback was fitted to $f(x)=ax^{-n}$. The positive feedback case in Figure 5E was fitted to a cubic polynomial with very high confidence (adjusted R^2=1). The distribution of intensity for the four models (Figure 6G) was calculated for a population of overexpressed network (five-fold). The population was assumed to have a uniform time distribution within a time interval $[t_0,3t_0]$, where t_0 is the time in which the wild-type network reaches 90% degradation. The Matlab Imagesc function was used to import 20 Tiff files of *Drosophila* embryos for quantitative analysis. Yan staining was calculated for 117 cells expressing ectopic Yan within the degradation border, and for 283 cells expressing ectopic Yan outside the border by averaging the amplitudes over dozens of pixels within each cell and normalizing by the background fluorescence of the embryo. The mean level of Yan overexpression was obtained by dividing the average value of the latter 283 cells by the average endogenous Yan value for 246 cells lying outside the degradation zone and the *prd* stripes. For Yan^D, 232 cells within the degradation border and 662 cells outside the degradation border were monitored. See Supplementary information for analytical derivations.

Supplementary information

Supplementary information is available at the *Molecular Systems Biology* website (www.nature.com/msb).

Acknowledgements

We thank D Baker, D Ish-Horowicz, C Klambt, I Rebay and J Skeath for generously providing reagents. We thank Rachel Tsruya for help and reagents, Shari Carmon for help and Eyal Schejter for advice and critical reading of the manuscript. This work was funded by grants from the Israel Science Foundation and the MD Moross Institute for Cancer Research (to BS) and from Israel Science Foundation and Minerva Foundation (to NB). GJM was a recipient of an EMBO long-term fellowship, NB is an incumbent of the Soretta and Henry Shapiro career development chair and BS is an incumbent of the Hilda and Cecil Lewis professorial chair in Molecular Genetics.

References

Baker DA, Mille-Baker B, Wainwright SM, Ish-Horowicz D, Dibb NJ (2001) Mae mediates MAP kinase phosphorylation of Ets transcription factors in *Drosophila*. *Nature* **411:** 330–334

Driever W, Nusslein-Volhard C (1988) The bicoid protein determines position in the *Drosophila* embryo in a concentration-dependent manner. *Cell* **54:** 95–104

Ferrell Jr JE (2002) Self-perpetuating states in signal transduction: positive feedback, double-negative feedback and bistability. *Curr Opin Cell Biol* **14:** 140–148

Gabay L, Scholz H, Golembo M, Klaes A, Shilo BZ, Klambt C (1996) EGF receptor signaling induces pointed P1 transcription and inactivates Yan protein in the *Drosophila* embryonic ventral ectoderm. *Development* **122:** 3355–3362

Gabay L, Seger R, Shilo BZ (1997) *In situ* activation pattern of *Drosophila* EGF receptor pathway during development. *Science* **277:** 1103–1106

Goldbeter A, Koshland Jr DE (1981) An amplified sensitivity arising from covalent modification in biological systems. *Proc Natl Acad Sci USA* **78:** 6840–6844

Goldbeter A, Koshland Jr DE (1984) Ultrasensitivity in biochemical systems controlled by covalent modification. Interplay between zero-order and multistep effects. *J Biol Chem* **259:** 14441–14447

Goldbeter A, Wolpert L (1990) Covalent modification of proteins as a threshold mechanism in development. *J Theor Biol* **142:** 243–250

Golembo M, Raz E, Shilo BZ (1996a) The *Drosophila* embryonic midline is the site of Spitz processing, and induces activation of the EGF receptor in the ventral ectoderm. *Development* **122:** 3363–3370

Golembo M, Schweitzer R, Freeman M, Shilo BZ (1996b) Argos transcription is induced by the *Drosophila* EGF receptor pathway to form an inhibitory feedback loop. *Development* **122:** 223–230

Gorlich D, Kutay U (1999) Transport between the cell nucleus and the cytoplasm. *Annu Rev Cell Dev Biol* **15:** 607–660

Jiang J, Levine M (1993) Binding affinities and cooperative interactions with bHLH activators delimit threshold responses to the dorsal gradient morphogen. *Cell* **72:** 741–752

Lai ZC, Rubin GM (1992) Negative control of photoreceptor development in *Drosophila* by the product of the *yan* gene, an ETS domain protein. *Cell* **70:** 609–620

O'Neill EM, Rebay I, Tjian R, Rubin GM (1994) The activities of two Ets-related transcription factors required for *Drosophila* eye development are modulated by the Ras/MAPK pathway. *Cell* **78:** 137–147

Qiao F, Song H, Kim CA, Sawaya MR, Hunter JB, Gingery M, Rebay I, Courey AJ, Bowie JU (2004) Derepression by depolymerization; structural insights into the regulation of *yan* by *mae*. *Cell* **118:** 163–173

Rebay I, Rubin GM (1995) Yan functions as a general inhibitor of differentiation and is negatively regulated by activation of the Ras1/MAPK pathway. *Cell* **81:** 857–866

Reeves GT, Kalifa R, Klein DE, Lemmon MA, Shvartsman SY (2005) Computational analysis of EGFR inhibition by Argos. *Dev Biol* **284:** 523–535

Song H, Nie M, Qiao F, Bowie JU, Courey AJ (2005) Antagonistic regulation of Yan nuclear export by Mae and Crm1 may increase the stringency of the Ras response. *Genes Dev* **19:** 1767–1772

Struhl G, Struhl K, Macdonald PM (1989) The gradient morphogen bicoid is a concentration-dependent transcriptional activator. *Cell* **57:** 1259–1273

Tootle TL, Lee PS, Rebay I (2003) CRM1-mediated nuclear export and regulated activity of the Receptor Tyrosine Kinase antagonist YAN require specific interactions with MAE. *Development* **130:** 845–857

Vivekanand P, Tootle TL, Rebay I (2004) MAE, a dual regulator of the EGFR signaling pathway, is a target of the Ets transcription factors PNT and YAN. *Mech Dev* **121:** 1469–1479